

ACCEPTED VERSION

Jing Li, Mark Thyer, Martin Lambert, George Kuczera, Andrew Metcalfe
An efficient causative event-based approach for deriving the annual flood frequency distribution

Journal of Hydrology, 2014; 510:412-423

© 2014 Elsevier B.V. All rights reserved.

This manuscript version is made available under the CC-BY-NC-ND 4.0 license
<http://creativecommons.org/licenses/by-nc-nd/4.0/>

Final publication at <http://dx.doi.org/10.1016/j.jhydrol.2013.12.035>

PERMISSIONS

<http://www.elsevier.com/about/company-information/policies/sharing#acceptedmanuscript>

[Accepted manuscript](#)

Authors can share their accepted manuscript:

[...]

After the embargo period

- via non-commercial hosting platforms such as their institutional repository
- via commercial sites with which Elsevier has an agreement

In all cases accepted manuscripts should:

- link to the formal publication via its DOI
- bear a CC-BY-NC-ND license – this is easy to do, [click here](#) to find out how
- if aggregated with other manuscripts, for example in a repository or other site, be shared in alignment with our [hosting policy](#)
- not be added to or enhanced in any way to appear more like, or to substitute for, the published journal article

Embargo

<i>ISSN</i>	<i>Journal Name</i>	<i>Embargo Period (months)</i>
0022-1694	Journal of Hydrology	24

7 June 2016

<http://hdl.handle.net/2440/84094>

An efficient causative event-based approach for deriving the annual flood frequency distribution

by

Li, J., Thyer, M., Lambert, M., Kuczera, G., Metcalfe, A.

Journal of Hydrology

Citation:

Li, J., Thyer, M., Lambert, M., Kuczera, G., Metcalfe, A. (2014). An efficient causative event-based approach for deriving the annual flood frequency distribution, Journal of Hydrology, Vol. 510, 412 – 423.

For further information about this paper please email Martin Lambert at Martin.Lambert@adelaide.edu.au

An efficient causative event-based approach for deriving the annual flood frequency distribution

Jing Li^a, Mark Thyer^a, Martin Lambert^a, George Kuczera^b, Andrew Metcalfe^c

*^aSchool of Civil, Environmental & Mining Engineering, the University of Adelaide
Engineering North N136, North Terrace Campus, the University of Adelaide, SA 5005,
Australia*

*jing.li06@adelaide.edu.au
+61 8 8313 1113*

*^bSchool of Engineering, University of Newcastle
ES Building - ES408, University of Newcastle, University Drive, Callaghan NSW 2308
Australia*

*^cSchool of Mathematical Sciences, the University of Adelaide
School of Mathematical Sciences, North Terrace Campus, the University of Adelaide, SA
5005 Australia*

Abstract

In ungauged catchments or catchments without sufficient streamflow data, derived flood frequency methods are often applied to provide the basis for flood risk assessment. The most commonly used event-based methods, such as design storm and joint probability approaches are able to give fast estimation, but can also lead to prediction bias due to the limitations of inherent assumptions and difficulties in obtaining input information (rainfall and catchment wetness) related to events that cause extreme floods. An alternative method is a long continuous simulation which produces more accurate predictions, but at the cost of massive computational time. In this study a hybrid method was developed to make the best use of both event-based and continuous approaches. The method uses a short continuous simulation to provide inputs for a rainfall-runoff model running in an event-based fashion.

The total probability theorem is then combined with the peak over threshold method to estimate annual flood distribution. A synthetic case study demonstrates the efficacy of this procedure compared with existing methods of estimating annual flood distribution. The main advantage of the hybrid method is that it provides estimates of the flood frequency distribution with an accuracy similar to the continuous simulation approach, but with dramatically reduced computation time.

Keywords:

Flood distribution estimation, Design Storm, Stratified Monte Carlo technique, Rainfall-runoff process, Continuous simulation, Peak over threshold method

1. Introduction

1 Flooding is one of the most frequently occurring natural hazards world-
2 wide, and often causes major damage to our society. For example, every year
3 in Australia, floods incur millions of dollars damage to critical infrastructure
4 and threaten humans lives. Appropriate designs of flow regulation structures,
5 such as dam spillways, bridges, pipelines and flood detention basins are vital
6 for flood mitigation and the protection of important domestic and commer-
7 cial resources. These designs rely on the estimation of both the frequency and
8 the magnitude of extreme flow events. However, due to the highly variable
9 and complex climatic and hydrological processes that drive flood extremes,
10 it is a major challenge to provide reliable predictions.

12

13 Existing flood estimation methods can be broken down into two ma-

14 jor groups: flood frequency analysis and derived flood frequency methods
15 (Moughamian et al. (1987)).

16

17 *1.1. Flood frequency analysis*

18 Flood frequency analysis involves fitting a distribution model to stream-
19 flow data so that the flow magnitude associated with a certain occurrence
20 probability can be calculated using the mathematical equation of the fitted
21 distribution. The success of the analysis depends on achieving a reliable
22 fit for the distribution, which requires a sufficiently long and high quality
23 streamflow record. Unfortunately it is not available in the vast majority of
24 catchments. Furthermore if the catchment has undergone significant land-
25 use or climate changes in the past, the historical record cannot support an
26 accurate estimation of the flood frequency distribution.

27

28 *1.2. Derived flood frequency methods*

29 Derived flood frequency methods have been developed to overcome the
30 limitations of flood frequency analysis. These approaches use meteorological
31 data (rainfall, potential evapotranspiration) as inputs for a rainfall-runoff
32 (RR) model to generate streamflow data. In general, historical rainfall data
33 are longer and have more reliable records than streamflow data and only a
34 relatively short streamflow record is required to calibrate the RR model. Fur-
35 thermore, to provide projections of the impact of climate change, a weather
36 generator can be used to simulate the meteorological data for a certain cli-
37 mate scenario. The simulated meteorological data is then input into the RR

38 model to generate streamflow data, from which the flood frequency distribu-
39 tion (FFD) under the projected climate condition can be derived. Derived
40 flood frequency methods are, therefore, generally preferred over flood fre-
41 quency analysis, and have been developed as both analytical and simulation
42 approaches.

43

44 Analytical methods were initiated in the early 70s by Eagleson (1972).
45 The author derived the peak streamflow distribution from the distributions
46 of catchment and climate characteristics using a kinematic runoff model in an
47 idealised V-shaped flow plane. Further development of the analytical meth-
48 ods was achieved by other researches, e.g., Hebson and Wood (1982), James
49 and Robinson (1986)) and Raines and Valdes (1993).

50

51 Recently, numerical simulation methods for deriving flood frequency dis-
52 tribution have undergone considerable development. These simulation tech-
53 niques can be classified into two groups: continuous simulation (CS) (Calver
54 and Lamb (2000)) and event-based (EB) approaches (e.g Rahman et al.
55 (2002)). CS runs a weather generator and a RR model in parallel con-
56 tinuously to produce a time series of streamflow data from which the flood
57 frequency curve can be derived, while EB approaches focus on the events of
58 interest. These usually include rainfall events and catchment wetness condi-
59 tions that drive extreme flood events and are sampled from their distributions
60 to serve as inputs for the RR model that runs in an event-based fashion. The
61 averaged return intervals (ARI) of the generated flood events are associated
62 with the ARI of the input events based on certain assumptions.

63

64 In the following, two mainstream event-based (EB) approaches, i.e., the
65 design storm and the joint probability approaches will be reviewed, followed
66 by a brief discussion of continuous simulation (CS).

67

68 *1.2.1. Design storm approach*

69 Among the EB methods, the most widely adopted one in the guidelines
70 of the world practicing water resource institutions (for example, the Aus-
71 tralian Rainfall and Runoff AR&R Pilgrim (1987)) can be attributed to the
72 design storm (DS) approach, mainly because of its simplicity. This approach
73 involves design event rainfall generation, runoff production and hydrograph
74 formation. It assumes that a design rainfall event of a given ARI can be
75 converted to a design flood of the same ARI and it relies on the specification
76 of a rainfall loss (aka antecedent soil moisture deficit) as an indicator of the
77 catchment wetness condition. A fixed value, typically the median, is taken
78 to represent the rainfall loss/soil moisture deficit (AR&R Pilgrim (1987)),
79 which ignores its variability. This assumption (also called as ARI neutrality
80 assumption) can lead to significant prediction errors, as the rainfall-runoff
81 process is basically a joint probability problem (Kuczera et al. (2003)). For
82 example, a 1 in 100 year flood can be caused by a 1 in 50 year rainfall event
83 falling on a wet catchment or by a 1 in 200 year rainfall event falling on a dry
84 catchment (Michele and Salvadori (2002)). Thus it is important to capture
85 the interactions of antecedent soil moisture conditions and extreme rainfall
86 events.

87

88 In order to overcome the problems of the ARI neutrality assumption,
89 Camici et al. (2011) proposed to calibrate the antecedent soil moisture to
90 the value that produces a flood with the same ARI as that of the input
91 rainfall event. For each return period of the flood, a design soil moisture
92 value is calibrated using the result of a long-term CS as a reference. The
93 design soil moisture values are then regionalised as a function of the geo-
94 morphological characteristics of the catchment so that they can be applied
95 to ungauged catchments with similar characteristics. Given the popularity
96 of the DS approach and its major problem of defining the antecedent soil
97 moisture condition, the attempt to find the critical soil moisture value that
98 maintains ARI neutrality during the transformation from rainfall to runoff
99 seems to be practical. Walsh et al. (1991) undertook a similar study for
100 New South Wales in Australia. However the regionalisation showed huge
101 variability. This indicates the success of this method strongly depends on the
102 strength of regionalization. The other significant limitation of this approach
103 is that the design soil moisture is likely to undergo significant change under
104 climate change condition. The regionalised design soil moisture inputs are
105 therefore likely to produce unreliable estimates of the FFD.

106

107 *1.2.2. Joint probability approaches*

108 To account for the joint probability nature of the estimation of extreme
109 flood events, event-based Monte Carlo simulation techniques have been de-
110 veloped (Rahman et al. (2002)), in which the values of the input variables,
111 e.g., rainfall depth and antecedent soil moisture amount are sampled from
112 either their joint or independent distribution and input into the RR model

113 to generate a range of streamflow events. Using the *total probability theorem*
114 the exceedance probability of these events can be estimated (Rahman et al.
115 (2002)). To reduce the computational time, stratified Monte-Carlo (SMC)
116 techniques are used in Nathan et al. (2003), where the sampling procedure
117 of the input variables focuses selectively on the probabilistic range of interest.

118

119 The major challenge of these techniques is to obtain the correct input dis-
120 tributions from the causative events of the annual maximum extreme flows
121 that are of interest. These are very difficult to obtain because long-term
122 historical records with many extreme events are not readily available. More-
123 over, catchment soil moisture conditions are not routinely measured, which
124 requires calibrating a RR model to flood events. Currently, practical guide-
125 lines (e.g., RORB by Laurenson et al. (2010)) recommend using the distri-
126 bution of annual maximum rainfall and some documented rainfall loss distri-
127 bution (e.g., Hill et al. (1997)) estimated from short historical data to derive
128 the annual FFD. Part of this study will evaluate the use of these practical
129 guidelines in the EB approaches for estimating the annual FFD.

130

131 As these procedures use the annual maximum rainfall as input and take
132 into account the joint probability of rainfall and catchment antecedent soil
133 moisture condition, we will collectively name these methods as AMXJP
134 methods hereafter, where *AMX* stands for annual maximum rainfall and
135 *JP* stands for joint probability.

136

137 *1.2.3. Continuous simulation*

138 In contrast to event-based approaches, continuous simulation (CS) (Calver
139 and Lamb (2000)) seems to solve all the problems mentioned above, under
140 the assumption that the applied weather generator and RR model adequately
141 simulate the rainfall-runoff process. It does not postulate ARI neutrality
142 between rainfall and runoff, nor does it require estimation of the input dis-
143 tributions for an EB procedure. It simply runs a weather generator coupled
144 with a RR model in a continuous manner to simulate a long time series of
145 streamflow data, from which the annual maximum flows can be extracted
146 and in turn the annual FFD can be derived.

147

148 The major limitation of the CS approach is that it is computationally
149 demanding. For instance, as will be shown in Sec. 4.4.2, to get an estimate
150 of the exceedance probability of 1 in 100 year flood with a prediction error
151 less than 20%, the minimum length of the simulated streamflow data needs
152 to be more than 9,500 years at a daily time step. If a complicated RR model,
153 such as a distributed and/or physically based model is required, the compu-
154 tational time can be prohibitive.

155

156 *1.3. Contribution of this work*

157 The main contribution of this paper is to develop a hybrid event-based
158 approach which overcomes the limitations of current EB approaches with
159 a significantly reduced computational time compared with a long-term CS.
160 This hybrid method uses a short CS run (e.g. 30-100 years) to provide input
161 distributions into an EB approach. As this method explicitly uses concur-

162 rent input events that are the true causative events of the output flows, it is
163 named as the *hybrid-causative events* approach (hybrid-CE). A key innova-
164 tion is that the EB approach is combined with the *total probability theorem*
165 to produce a so-called *event streamflow distribution*, which is converted to
166 the annual FFD using the peak over threshold (POT) method. This enables
167 improvement in the accuracy of the predictions of the annual FFD compared
168 with the existing EB approaches, and a remarkable enhancement in compu-
169 tation efficiency compared with a long-term CS.

170

171 The paper is organised as follows: Section 2 outlines the hybrid-CE
172 methodology. Section 3 presents a synthetic case study to demonstrate the
173 advantages of the hybrid technique over the existing EB approaches men-
174 tioned above, i.e., the DS and AMXJP methods. Section 4 provides the
175 results, which illustrate how the limitations of the DS and AMXJP methods
176 produce significant errors in the estimation of annual FFD and then demon-
177 strates the accuracy of the hybrid-CE method. The final part of section 4
178 compares the three different approaches. Section 5 provides some discussion
179 of relevant issues, including future research topics. Section 6 provides the
180 summary and conclusions.

181

182 **2. Development of the Hybrid-CE Approach**

183 The hybrid-CE approach combines continuous simulation and event-based
184 approaches. A long CS of rainfall provides the rainfall distribution and a
185 short CS of the rainfall-runoff process provides the soil moisture distribu-

186 tion. Together, they drive an EB simulation of the rainfall-runoff process
187 to produce the streamflow distribution. Unlike the AMXJP method, for
188 the hybrid-CE method the input rainfall and soil moisture values are drawn
189 from the distributions that are estimated from causative events to produce
190 an *event streamflow distribution*. The POT method is then applied to con-
191 vert this distribution to the annual FFD.

192

193 A schematic diagram shown in Fig. 1 illustrates the interactions between
194 different components of the hybrid-CE method. The following sections ex-
195 plain the three major components (continuous part, event-based part and
196 FFD conversion part) one by one in details. This method is generic and
197 can be adapted to provide estimates of the distribution of extremes for the
198 events of interest, e.g., either instantaneous peak flow rates or event volumes.
199 For the purposes of demonstrating the value of the hybrid-CE method, we
200 chose the simplest case study, which is to estimate daily streamflow extremes
201 using daily rainfall depth and antecedent soil moisture. Sec. 5.2 discusses
202 future extensions to the hybrid-CE method to estimate the more practically
203 relevant distribution of extremes of the instantaneous peak flow rate.

204

205 In the following discussions, the capital letters R , S and Q denote the
206 random variables representing rainfall, soil moisture and streamflow, respec-
207 tively and small letters r , s and q the corresponding variates. The capital
208 letter $F()$ is used to denote the cumulative distribution function, while the
209 small letter $f()$ is used to denote the probability density function.

210

211 *2.1. The continuous part*

212 Although rainfall records are more numerous than streamflow records,
213 they may not be available at the time scale or location of interest. In gen-
214 eral, stochastic rainfall models (for example Cowpertwait (2006)) can be used
215 to circumvent limitations of rainfall records and provide the required long-
216 term rainfall simulations.

217

218 As in the event-based part of the hybrid-CE method the rainfall distribu-
219 tion is needed, the continuous part of the hybrid-CE approach first runs the
220 rainfall simulation to generate a long-term rainfall record based on the as-
221 sumption that the rainfall simulation runs much faster than the RR model.
222 The grounds for this assumption will be addressed in Sec. 3.5. Thus the
223 rainfall distribution can be estimated from this long-term record which cov-
224 ers more extreme events than the observed data, or under climate change
225 conditions, predicts the rainfall in the future in a probabilistic sense.

226

227 After that a short-term continuous simulation of the RR model is run
228 using part of the generated long rainfall record as input. From this short
229 term CS of the RR process, a short time series of soil moisture values as well
230 as streamflow values are obtained. Given that soil moisture are less variable
231 than rainfall, this short record of the soil moisture is sufficient for the esti-
232 mation of its distribution. The short streamflow record will be used to assess
233 the POT model parameters, as will be discussed in Sec. 2.3.

234

235 *2.2. The event-based part*

236 After obtaining the rainfall and soil moisture distributions, their values
237 (r and s) can be sampled to be input into the RR model. For each EB run of
238 the RR model, a streamflow value (\hat{q}) is generated. This value is compared
239 to the streamflow value of interest (q). Note that, in general, q can be ei-
240 ther an instantaneous flow rate at a given point in time or the volume over
241 a given time period during which the amount of rainfall and soil moisture
242 are accumulated. As noted earlier, we chose to adopt the simpler case of
243 the daily flow volume to exemplify the method. A follow-up discussion on
244 the extension of the method to estimate the more complicated case, i.e., the
245 instantaneous flow rate, is provided in Sec. 5.2.

246

247 Assuming that the RR model is deterministic, with no prediction error,
248 the conditional exceedance probability of the streamflow conditioned on the
249 rainfall and soil moisture values, $P(Q > q|r, s)$, can be evaluated:

$$P(Q > q|r, s) = \begin{cases} 1 & \text{if } \hat{q} > q \\ 0 & \text{if } \hat{q} \leq q \end{cases} \quad (1)$$

250 In reality, RR models can have significant predictive errors due to data
251 and model structural errors (see Thyer et al. (2009) and Renard et al. (2010)
252 for further discussions). If a prediction error is introduced into the RR model,
253 the value of $P(Q > q|r, s)$ will range between 0 and 1. For the current study,
254 we assume the RR model is deterministic.

255

256 Based on the total probability theorem, the unconditional exceedance
257 distribution $1 - F(q)$ of the streamflow can be calculated by:

$$\begin{aligned}
1 - F(q) &= \int_{\Omega_R} \int_{\Omega_S} (1 - F(q|r, s))f(r, s)dsdr \\
&= \int_{\Omega_R} \int_{\Omega_S} P(Q > q|r, s)f(r|s)f(s)dsdr \quad (2)
\end{aligned}$$

258 where $f(r, s)$ denotes the joint probability density of rainfall and soil mois-
259 ture, while $f(s)$ stands for the rainfall probability density obtained from the
260 long-term rainfall simulation and $f(r|s)$ denotes the conditional probability
261 density of soil moisture conditioned on rainfall, which is obtained through
262 the short-term CS of the RR model. It is worth mentioning that if r and s
263 are independent, $f(r, s)$ can be broken down into $f(r) \cdot f(s)$. $F(q|r, s)$ de-
264 notes the cumulative conditional distribution of streamflow conditioned on
265 the input r and s values. $P(Q > q|r, s)$ is evaluated in Eq. (1).

266

267 The double integral in Eq. (2) can be computed through Monte Carlo
268 integration (Davis and Rabinowitz (1975)). Nathan et al. (2003) developed
269 the stratified Monte-Carlo (SMC) method which improves the calculation
270 efficiency by using stratified sampling of the input values on the probabilistic
271 range of interest.

272

273 In the hybrid-CE method, we developed an efficient numerical integration
274 for extreme events (ENIEE) to solve Eq. (2), where the pairing of r and s is
275 done on a grid of the domain $Dom = R \times S$. Using ENIEE Eq. (2) becomes:

$$1 - F(q_k) = \sum_i^n \sum_j^n P(q_{ij} > q_k|r_i, s_j)f(r_i, s_j)\Delta s\Delta r \quad (3)$$

276 Compared to the SMC technique, the ENIEE is more efficient, as the
277 input r and s values are checked in an ordered manner so that it is easy
278 to terminate further evaluations of the RR model at any point of (r_i, s_j)
279 that does not contribute to the q_k value under investigation. For the SMC
280 method, on the other hand, the program has to wait until all the random
281 samplings within the specific intervals are finished. A detailed description of
282 the ENIEE is provided in the Appendix.

283

284 Like the AMXJP methods, the mathematical theory underpinning the
285 event-based part of the hybrid-CE method is also the *total probability theo-*
286 *rem.* However the major difference lies in the fact that the AMXJP methods
287 uses the annual maximum rainfall and user-defined soil moisture events (see
288 Sec. 1.2.2) to assess the input distributions for the calculation of the annual
289 FFD. In contrast, the hybrid-CE method uses the rainfall and soil moisture
290 events that are truly concurrent/causative to the streamflow events at the
291 event temporal scale of interest. For example, if the event temporal scale of
292 the streamflow is daily/hourly, then the input rainfall and soil moisture distri-
293 butions will be evaluated through the daily/hourly rainfall and soil moisture
294 events, respectively.

295

296 Hence the term $F(q_k)$ in Eq. 3 becomes the distribution of streamflows
297 at the event temporal scale of interest (referred to as *event streamflow dis-*
298 *tribution* hereafter). Then the POT method is incorporated to convert this
299 distribution to the annual FFD, which will be introduced in the next section.

300

301 One may argue that the *event streamflow distribution* can be directly esti-
302 mated from the output streamflow data of the short CS run of the RR model
303 and that is therefore unnecessary to use the EB simulation of the RR process
304 and the ENIEE method. However, the short time series of the rainfall data
305 that drive the RR model for a short CS run may not contain enough extreme
306 events of major interest. Therefore, the short series of streamflow data gen-
307 erated by the short CS can lead to enormous uncertainties in the subsequent
308 estimation of the extreme events in the annual maximum flow series, whereas
309 in the EB component of the hybrid-CE method, the input rainfall events are
310 drawn from the distribution which is estimated from the long-term rainfall
311 record where more extreme events are present. Therefore the resultant *event*
312 *streamflow distribution* is more reliable for use in the subsequent derivation
313 of the annual FFD.

314

315 *2.3. Derivation of the annual FFD using the POT method*

316 The POT method (Shane and Lynn (1964) and Todorovic and Zelenhasic
317 (1970)) is often applied in flood frequency studies as an alternative to the
318 annual maximum series (AMS) method. A comprehensive discussion on the
319 POT method can be found in Rosbjerg (1993). As the current study was
320 focused on the estimation of annual FFD, we continued seeking the distribu-
321 tion of annual maximum flows. The POT method was adopted as a tool to
322 derive the annual FFD from the *event streamflow distribution*.

323

324 In the POT method, the number of peaks over the selected flow threshold
325 q_0 per year is considered as a random variable, the probability of which is

326 denoted by:

$$P(\text{w peaks} > q_0 \text{ in a year}) = P_w \quad (4)$$

327 Under the assumption that the peak magnitudes are independent and
 328 identically distributed (i.i.d) with function $F(Q \leq q|q \geq q_0)$, the distribution
 329 of the annual maximum flows (Q_a) can be calculated by (Todorovic and
 330 Zelenhasic (1970)):

$$F_{Q_a}(Q_a \leq q) = \sum_{w=0}^W P_w (F(Q \leq q|q \geq q_0))^w \quad (5)$$

331 where W denotes the number of basic time steps (e.g., daily or hourly) in
 332 a year, depending on the measurement temporal resolution or the event time
 333 scale of interest. The probability distribution of the number of peaks exceed-
 334 ing the threshold per year (P_w) is often modeled by the Poisson distribution
 335 (Rosbjerg (1993)). However Cunnane (1979) suggests that the negative bin-
 336 omial distribution is more suitable for a POT series which exhibits great
 337 variability. In the current study (Sec. 3.5.3), it was found that a negative bi-
 338 nomial distribution fits better to the data, hence it was adopted to the model
 339 the P_w and thus Eq. (5) becomes:

$$\begin{aligned} F_{Q_a}(q) &= \sum_{w=0}^W \frac{\Gamma(\gamma + w)}{w! \Gamma(\gamma)} (1-p)^\gamma p^w (F(Q \leq q|q \geq q_0))^w \\ &= (1-p)^\gamma (1 - F(q|q \geq q_0)p)^{-\gamma} \end{aligned} \quad (6)$$

340 where p and γ are parameters of the negative binomial distribution. Note
 341 that $F(q|q \geq q_0)$ is a truncated distribution and the following relationship
 342 holds true:

$$F(q|q \geq q_0) = \frac{F(q)}{1 - F(q_0)} \quad (7)$$

343 where $F(q)$ is the *event streamflow distribution* which was defined in Sec.
 344 2.2. The denominator $1 - F(q_0)$ is a normalizing factor. The problem of
 345 estimating the input distribution of annual concurrent events is therefore
 346 reduced to estimating the distribution of the input variables in accordance
 347 with the event time scale of interest. In other words, the extraction of the
 348 annual causative events from a long data series is no longer necessary and the
 349 distribution of the input variables can be much more easily obtained either
 350 through measurements or a short CS run.

351

352 2.4. Summary of the hybrid-CE approach

353 In summary, the hybrid-CE approach requires the following steps:

- 354 1. A long-term CS is run for the rainfall simulation at the streamflow
 355 event time scale of interest to generate a long time series of rainfall
 356 data. The rainfall distribution is estimated from this record.
- 357
- 358 2. A short rainfall record sampled from the simulated data is put into
 359 the RR model for a short-term CS run at the same event time scale to
 360 generate a series of soil moisture values for the estimation of the soil
 361 moisture distribution. The streamflow record generated by the short
 362 CS is used to estimate the POT model parameters (q_0 , p and γ in Eq.
 363 (6)).

364

365 3. The RR model is run in an event-based manner using the rainfall and
366 soil moisture values sampled from the estimated distributions and the
367 ENIEE method is implemented to evaluate the *event streamflow dis-*
368 *tribution* using Eq. (3).

369

370 4. The POT method is applied to convert the *event streamflow distribu-*
371 *tion* to the annual FFD using Eq. (5).

372

373 The flow chart of the above steps is illustrated in Fig. 1.

374

375 **3. Case Study**

376 In order to demonstrate how the assumptions of the DS and AMXJP ap-
377 proaches produce biases in their estimation of the annual FFD, a synthetic
378 case study was developed. In this section, the case study is described to show
379 that the hybrid-CE approach overcomes these biases and provides more reli-
380 able estimates of the annual FFD in an efficient manner.

381

382 The rainfall data of the synthetic catchment were generated through a
383 1-D continuous rainfall simulation model. The simulated rainfall data were
384 input into a lumped RR model to generate a long-term (10,000 years) se-
385 quence of daily streamflow values in order to derive the *virtual truth* annual
386 FFD for comparison purpose.

387

388 Simple lumped rainfall and RR models were applied in this case study,
389 because the aim was to show the problems of the existing approaches and
390 the relative efficacy of the hybrid-CE method. Extensions of the hybrid-CE
391 method to a more complicated RR model using realistic catchment data will
392 be undertaken in future research (see Sec. 5.2), after the effectiveness of the
393 method has been established using simple 1-D models in this study.

394

395 *3.1. Rainfall simulation model*

396 The daily rainfall simulation model consists of two parts: an occurrence
397 model for the generation of dry-and-wet-day sequence and a model for the
398 generation of rainfall amount on wet days (Srikanthan and McMahon (2001)).

399

400 The dry/wet day sequence is modeled by a first order stationary Markov
401 chain (Weiss (1964)), the parameters of which are the initial/stationary wet-
402 day probability P_{W0} and two conditional probabilities P_{WW} (the probability
403 of a wet day given that the previous day was wet) and P_{DW} (the probability
404 of a wet day given the previous day was dry).

405

406 The rainfall amount on wet days in the case study was drawn from a
407 log-normal distribution with parameter values $\mu = 1.5$, $\sigma = 1.0$.

408 *3.2. Rainfall-runoff model*

409 The applied RR model is a simplified HBV model (Bergström (1995))
410 with the snow and the dual-reservoir modules omitted. The snow module

411 was eliminated in order to illustrate a technique that focuses on extreme rain-
412 fall driven peak flow events, rather than snow-melt driven (or rain-on-snow)
413 peak flow events, as these types of events are rare in Australia. The reser-
414 voir module was removed because this study was focussed on the frequency
415 distribution of extreme flows. The recession part of the hydrograph which is
416 emulated by the reservoir module is not essential to the problem.

417

418 *3.3. Climate scenarios*

419 To test the performance of different EB approaches under different cli-
420 mate conditions, a wet and a dry climate scenarios were generated using
421 different parameter settings for the rainfall simulator and HBV model. The
422 selection of the parameters for the two climate scenarios was based on a
423 comparison of the annual rainfall and runoff statistics from a database of
424 330 Australia catchments (Peel et al. (2000)). The wet/dry climate scenario
425 was assigned an annual mean rainfall in the upper/lower 1% of the Peel et al.
426 (2000) dataset. Table (1) summarizes the annual statistics of the two climate
427 scenarios.

428

429 *3.4. Virtual truth reference for the annual FFD*

430 After the model setup, a 10,000-year continuous simulation of the rainfall
431 and rainfall-runoff models was carried out at a daily time step for both cli-
432 mate scenarios. As metioned at the beginning of the case study, the output
433 streamflow data were used to derive the *virtual truth* annual FFD, which was

		Annual Max [mm]	Annual Min [mm]	Annual Mean [mm]	CV [-]	Annual POE [mm]
Dry	rainfall	1468.18	258.98	674.67	0.20	1277
	discharge	249.69	2.61	32.91	0.57	
Wet	rainfall	2452.59	928.26	1540.76	0.11	1387
	streamflow	998.98	103.62	321.06	0.27	

Table 1: Summary of the annual statistics of the two climate scenarios. CV stands for the coefficient of variance for the annual sums.

434 used to evaluate the results of the different methods tested in the following.

435

436 3.5. Input information

437 In EB joint probability approaches, distribution of the input rainfall is
438 required. The advantage of fast rainfall simulation technique can be uti-
439 lized to generate a long rainfall record for a better estimation of the required
440 rainfall distribution. Therefore in this case study, access to the long-term
441 rainfall record (10,000 years of daily values) and a short streamflow record
442 (e.g., 30-100 years of daily values) were assumed. The difference in the acces-
443 sible record lengths was based on the assumption that the rainfall simulation
444 would be much faster than the simulation of the rainfall-runoff process. A
445 space-time rainfall model using the circulant embedding method and fast
446 Fourier transformation needs just one second to simulate a 512×512 image
447 (Qin (2010)). In contrast, it can take hours to run a 2D hydrodynamic model
448 at a smaller spatial resolution (Neal et al. (2009)).

449

450 3.5.1. DS approach

451 Based on the ARI neutrality assumption of the DS approach, annual
452 maximum rainfalls should be used as inputs into the RR model to derive the
453 annual FFD. In this case study, the annual maximum rainfalls were extracted
454 from the simulated 10,000-year daily rainfall series.

455

456 Regarding the antecedent catchment wetness condition, the primary as-
457 sumption of the DS approach is that it uses a single fixed representative loss
458 value. Typically, a rainfall loss model (e.g. proportional, initial/continuing)
459 and a runoff routing procedure are used to convert rainfall to runoff (e.g.
460 Laurenson et al. (2010)). Traditionally the representative value of the initial
461 loss is taken as the median of some documented distribution assessed from
462 historical data. In Hill et al. (1997), the distribution of the initial loss are
463 calibrated based on the rainfall events from a POT series (events with ARI
464 greater than one year) and their concurrent flow events. The continuing loss
465 value is determined through mass balance.

466

467 For this case study we used the simplified HBV model to convert rainfall
468 to runoff in the DS approach because it was exactly the same RR model used
469 to generate the *virtual truth* FFD. This enabled us to specifically test the im-
470 pact of assessing a single representative antecedent catchment wetness value,
471 without introducing errors due to the ability of the RR model to represent
472 the *virtual truth*. Thus a single representative antecedent soil moisture (SM)
473 value was used, as it plays the same role in the HBV model as the rainfall

474 loss in a routing model. The rainfall threshold was evaluated based on the
475 10,000-year daily rainfall record. Then, with the short daily records (100
476 years), the soil moisture values prior to the rainfall events that are above the
477 threshold were selected to estimate the SM distribution. Finally the median
478 SM value was calculated from this distribution as the representative value.

479

480 3.5.2. *AMXJP method*

481 For the AMXJP methods such as Nathan et al. (2003), the design guide-
482 lines, e.g., RORB by Laurenson et al. (2010), recommend that the input
483 variables (rainfall and soil moisture) are treated as independent variables.
484 Thus the term $f(r, s)$ in Eq. (3) becomes $f(r) \cdot f(s)$. For the rainfall distri-
485 bution, the distribution of annual maxima is used (Nathan et al. (2003)). In
486 this case study, this distribution is estimated from annual maximum rainfalls
487 extracted from the 10,000-year daily rainfall data.

488

489 It is recommended that the loss distribution is taken from the documented
490 distribution as described in Hill et al. (1997) (Nathan et al. (2003), Lauren-
491 son et al. (2010)). This is the same as used by the DS approach to obtain
492 the representative value. Therefore the soil moisture distribution estimated
493 for the DS approach in the previous section was used to test the AMXJP
494 method in this study.

495

496 *3.5.3. Hybrid-CE method*

497 In the application of the hybrid-CE method, first the dependence be-
498 tween the daily rainfall depth and soil moisture amount was investigated
499 using Pearson's ρ , Spearman's ρ and empirical copulas (Nelsen (2006)) as
500 measures of dependence. No significant dependence was found. Therefore
501 as in the AMXJP method, the individual distributions of rainfall and soil
502 moisture were used. The distribution of the daily rainfall depth was directly
503 assessed from the entire 10,000-year daily rainfall record. The distribution
504 of the daily soil moisture conditions was estimated using the 100-year daily
505 SM record sampled from the long-term daily SM record (10,000 years).

506

507 In addition to the input distributions, the occurrence model of the peaks
508 over threshold and its parameters have to be specified for the POT method
509 to convert the daily flow distribution to the annual FFD.

510

511 First of all, the peak threshold should be chosen. Rosbjerg (1987) pointed
512 out that a flow threshold that corresponds to a yearly occurrence number ex-
513 ceeding 5 leads to a significant positive correlation between the peak magni-
514 tudes which violates the basic assumption of the POT method. On the other
515 hand, too small value of the occurrence rate limits the number of events in a
516 short record for statistical analysis. Therefore in this study, a flow threshold
517 was chosen such that its average yearly occurrence number was 3.

518

519 Two different models of the occurrence rate of peaks were considered,
520 the Poisson and the negative binomial distributions. Visual inspection of

521 the frequency curves of the number of peaks per year from the 10,000 year
 522 streamflow record (not shown) showed that the negative binomial distribu-
 523 tion provided a better fit than the Poisson to the observed data. Table 2
 524 reports the results of the chi-squared test and confirms the above findings.

525

	Poisson			Negative Binomial		
	df	Chi-S	P-value	df	Chi-S	P-value
Dry	10	170270.3	0	24	22.1	0.57
Wet	10	26792.4	0	17	19.3	0.31

Table 2: *Result of the chi-squared test for the goodness of fit of the occurrence models. 'df' denotes the degree of freedom, 'Chi-S' denotes the chi-squared test statistics.*

526 Therefore the negative binomial distribution was adopted. The model
 527 parameters γ and p in Eq. (6) were estimated using the method of moments
 528 (Cunnane (1979)).

529

530 In the following application of the hybrid-CE approach, the POT model
 531 parameters (q_0 , p and γ) were assessed from the random samples of 100-year
 532 daily records of streamflow generated by the CS. This means for different
 533 random samples, different sets of POT model parameters were estimated.

534

535 **4. Results**

536 *4.1. DS approach*

537 Fig. 2 shows the predicted annual FFD from the DS approach for both
538 the wet and the dry climate scenarios compared to the *virtual truth* annual
539 FFD. Black curves indicate the *virtual truth* distributions. The light blue
540 curves *DS-100* indicate the results using randomly sampled 100-year records
541 (in total 100 independent records) to assess the representative SM value. In
542 addition, in order to check the model performance in a condition free from
543 sampling error, the entire 10,000-year record was used to derive the represen-
544 tative SM value, and the results *DS-10000* are shown by the dark blue curves.

545

546 The results highlight an overall under-estimation. For the very small
547 flood values, however, the DS approach produces a slight over-estimation.

548

549 *4.2. AMXJP approach*

550 Fig. 3 shows the results of the AMXJP approach. The curves represent-
551 ing *AMXJP-10000* and *AMXJP-100* have similar meanings as *DS-10000* and
552 *DS-100* described in Sec 4.1. The results show an averaged good agreement
553 with the *virtual truth*, but with relatively large estimation uncertainties.

554

555 The purple dashed lines representing the results of *JPCE-10000* indi-
556 cate the outcome of the joint probability method using input distributions
557 estimated from the causative events, i.e., rainfall and SM events that are
558 concurrent with/prior to the annual maximum flow events. They are also in

559 line with the *virtual truth*. The slight discrepancies are due to the fact that
560 the JPCE approach ignores the dependence between the causative rainfall
561 and SM events.

562

563 4.3. Hybrid-CE method

564 Fig. 4 shows the results of the hybrid-CE method. A relatively good
565 agreement between the average behaviour of the predictions using the short
566 records (*HCE-100*) and the *virtual truth* can be observed. The same ap-
567 plies to the predictions resulted from the use of the entire 10,000-year record
568 (*HCE-10000*).

569

570 4.3.1. Optimal short record for the hybrid-CE method

571 As shown above, the predictions of *HCE-10000* by the hybrid-CE method
572 are in line with the *virtual truth* distribution. But it relies on obtaining the
573 input daily SM distribution and the POT model parameters from the entire
574 10,000-year data records. That requires a long CS of the RR model. However,
575 as noted before, the aim of the hybrid-CE method is to avoid running a long
576 CS of the RR model, as it can be very computationally expensive. On the
577 other hand, using short records generated by a short CS of the RR model
578 for the estimation, due to sampling variability, the predicted distribution
579 can have large or small errors compared with the *virtual truth* distribution.
580 Therefore the question is whether certain statistics of the short record can
581 be found which selects a short record among the different random samples
582 so that the error in predicting the annual FFD due to random sampling is

583 minimized.

584

585 As stated in Sec. 3.5, it was assumed that a long-term rainfall record can
586 be simulated. The goal here was to choose a short (30-100 years) rainfall
587 record from the long rainfall record in order to produce a short CS of the
588 RR model from which the best estimates of the SM distribution and POT
589 parameters can be obtained. The selection of the short rainfall record was
590 determined by the match between the statistical properties of the short rain-
591 fall record and those of the long record.

592

593 Several statistics (daily mean, median, standard deviation and skewness)
594 and different record lengths were tested (30 to 100 years with an increment of
595 10 years). It was found that mean daily rainfall provided the best statistics
596 for selecting the short rainfall record.

597

598 Fig. 5 shows the results of using this approach for choosing the optimal
599 short record for the 30, 40 and 50-year record lengths. The values of RP
600 in Fig. 5 indicate the percentage of the random samples of short records
601 outperform the optimal short record. These figures and the low RP values
602 illustrate the fact that this method for choosing the optimal short record
603 provides a good match to the *virtual truth* distribution, even for the record
604 length of 30 years.

605

606 *4.4. Comparison of methods*

607 *4.4.1. Predictive ability*

608 Fig. 6 and 7 compare the 95% confidence limits and the averaged results
609 of the three methods for the dry and wet cases, respectively. They show that
610 the DS approach produced the worst performance. There are significant
611 under-estimations especially for the high annual maximum extreme flows.
612 This outcome demonstrates that using a fixed representative antecedent SM
613 value produces poor performance and highlights the importance of consider-
614 ing the variabilities of key input variables other than rainfall.

615

616 The AMXJP approach provided good predictive performance on average,
617 however, it produced the largest prediction uncertainties among the three
618 methods. This good performance was despite using arbitrarily chosen SM
619 distributions, that were not based on the causative events. Fig. 8 shows
620 that this good predictive performance was due to a compensation of errors
621 between the annual max rainfall distribution and SM distribution used by
622 AMXJP (similar effect is observed for the wet case which was not shown).
623 The AMXJP approach relies on this compensation of errors to produce re-
624 liable predictions of the annual FFD. A relevant question is whether this
625 compensation of errors applies only to this simplified case study and if it can
626 be relied upon over a large range of climate and catchment conditions.

627

628 The hybrid-CE method provided good predictive performance on average
629 except for a slight overestimation for the low flows in the dry case. The resul-
630 tant estimation uncertainty was smaller than for the AMXJP approach, but

631 higher than for the DS approach. The DS approach produces the narrowest
632 prediction band simply because it does not take into account the variability
633 of SM conditions like the other two methods. Despite the additional com-
634 plexities in the hybrid-CE method (estimating input distributions and POT
635 model parameters) compared with the AMXJP approach it produces smaller
636 prediction uncertainties. This demonstrates the relative robustness of the
637 hybrid-CE method. Note that the relative uncertainty due to sampling vari-
638 ability is greater in the dry case than in the wet case for all three methods.
639 This is likely to be because of the larger coefficients of variance of the rainfall
640 and runoff data (Table 1).

641

642 A comparison of the relative prediction errors of the three different meth-
643 ods for different record lengths is demonstrated by Fig. 9 and 10 which show
644 the probability distribution of the difference in the normalized root mean
645 square errors (NRMSE) normalized to the range of the true values from the
646 *virtual truth* distribution. The differences in the NRMSE were calculated
647 between the results of different methods. For example, to compare the per-
648 formance of the DS and the hybrid-CE approaches, the NRMSE_{DS} minus
649 $\text{NRMSE}_{\text{HCE}}$ was calculated, while to compare the AMXJP and hybrid-
650 CE approaches, the $\text{NRMSE}_{\text{AMXJP}}$ minus $\text{NRMSE}_{\text{HCE}}$ was calculated.
651 A positive NRMSE difference indicates that the hybrid-CE outperforms ei-
652 ther the DS or AMXJP. The probability distribution was based on 400, 200
653 and 100 independent replicates (from the 10,000-year record) for the differ-
654 ent record lengths of 25, 50 and 100 years, respectively. The percentage
655 of replicates with a positive NRMSE differences indicates the probability

656 that hybrid-CE outperforms either DS or AMXJP. Fig. 9 and 10 show that
657 hybrid-CE clearly outperforms DS (greater than 90% positive NRMSE differ-
658 ence for the dry case and 85% to 95% for the wet case), and also outperforms
659 the AMXJP approach for the dry case (60-70% positive NRMSE difference),
660 while there is only a marginal improvement in performance compared to the
661 AMXJP for the wet case (55-60% positive NRMSE difference).

662

663 These results indicate that if a single short record is randomly selected it
664 is likely that the hybrid-CE method will produce more accurate estimates of
665 the annual FFD than the DS and AMXJP approaches, particularly for the
666 dry case. In addition, Sec. 4.3.1 has shown that by selecting the optimal
667 short record for the hybrid-CE method the prediction error due to random
668 sampling of the short records is significantly reduced and the result is very
669 close to that of using the entire 10,000-year records. Overall, these results
670 clearly illustrate that the hybrid-CE method provides more reliable predic-
671 tions than both the DS and AMXJP approaches.

672

673 *4.4.2. Computational efficiency*

674 The previous section showed that the hybrid-CE method provides more
675 reliable predictions of the annual FFD than the DS and AMXJP methods.
676 The main advantage of the hybrid-CE approach over the long-term CS ap-
677 proach is its computational efficiency. For example, to achieve a prediction
678 error less than 20% for the exceedance probability of the 1 in 100 year flood
679 the required number of years n to be simulated in the CS at a daily time
680 step can be calculated according to the principle of Binomial proportion con-

681 fidence interval (Brown et al. (2001)):

682

$$1.96 \times \sqrt{\frac{\hat{p}(1 - \hat{p})}{n}} < 0.20\hat{p} \quad (8)$$

683 Eq. (8) shows that to achieve the desired prediction accuracy, the num-
684 ber of events which the RR model must simulate in the CS at a daily time
685 step is 3,470,420. In comparison, the hybrid-CE method needs only 1.4%
686 of the number of events to be simulated by the RR model, if 100 years of
687 daily CS run is required for estimating the SM distribution and the POT
688 parameters. If only 30 years of a CS run is sufficient to get this information,
689 the number of events which the RR model simulates can be further reduced
690 to 0.68% of that of the long CS run. This reduction in computational time
691 offers major advantages when a complicated distributed RR model such as
692 (Vischel et al. (2008)) or HydroGeoSphere (Therrien et al. (2010)) is required
693 to estimate the annual FFD. Table 3 compares the prediction accuracy and
694 computational efficiency of the different methods.

695

696 **5. Discussions**

697 *5.1. Comparing the hybrid CE approach against existing approaches*

698 The synthetic case study demonstrated that the hybrid-CE method out-
699 performs the traditional DS and AMXJP event-based methods in terms of
700 prediction accuracy. For the DS method, the ARI neutrality assumption and
701 the use of a fixed representative SM value lead to significant underprediction

Method	Relative computation time	Predictive Performance
DS	1	both over and under-estimation
AMXJP	100*	large prediction uncertainties, reliability based on arbitrary assumptions
CS	$10^4 - 10^6$	minimal bias, least uncertainty
HCE	100*	small bias, reduced uncertainty

Table 3: Comparison of the performance of different methods. *Long enough to manage the sampling error to acceptable level.

702 (13% to 46% for the dry case and 2.3% to 17% for the wet case on aver-
703 age) of the annual FFD. This under-estimation is due to a combination of
704 assuming a fixed value of the SM and the non-linear increase in event runoff
705 response when the SM increases. As the DS method is the most widely used
706 approach for estimating annual FFD, this is of major concern to flood engi-
707 neers who use this method. The study suggests that flood risks are currently
708 being under-estimated. The degree of this under-estimation will vary due to
709 catchment and climate conditions. For example in this simplified synthetic
710 case study, the relative errors in the dry case were far higher than errors in
711 the wet case study. These results should sound a warning for flood engineers
712 who use DS approaches.

713

714 For the AMXJP method, the use of the entire SM distribution resulted in
715 improved performance relative to the DS approach, but with a lower predic-
716 tive accuracy and higher predictive uncertainty than provided by the hybrid-

717 CE method (see Fig. 6, 7, 9 and 10). Another significant concern with the
718 AMXJP method is that it relies on the compensation of errors arising from
719 the use of an arbitrarily assumed SM distribution combined with the annual
720 maximum rainfall distribution to provide good predictive performance. In
721 the simplified synthetic case study this produced reasonable performance.
722 However, whether this is true, in a more realistic case study, using a more
723 realistic rainfall and RR model is an open question. A more realistic rain-
724 fall model would produce subdaily rainfall predictions, taking into account
725 seasonally varying wet and dry spell durations and rainfall intensities (e.g.
726 the DRIP model of Heneker et al. (2001)) and also inter-annual and multi-
727 decadal variability (e.g. CIMSS approach of Henley et al. (2011)). A more
728 realistic RR model would provide predictions of the subdaily flow, taking into
729 account the non-linear spatially varying catchment processes of infiltration
730 and soil moisture to generate baseflow, interflow and surface flow, which at
731 any time can contribute to the flood peak (e.g. TOPKAPI, Vischel et al.
732 (2008)). Given these complexities it is unclear that assuming an arbitrary
733 SM distribution based on a POT series of the rainfall would provide reli-
734 able predictive performance across a large range of catchment and climate
735 conditions. In contrast, the hybrid-CE is a conceptually sounder approach
736 because it uses the rainfall and SM distributions of the causative events that
737 produce the streamflow events to provide efficient and reliable estimates of
738 the annual FFD.

739

740 Another drawback of the DS and AMXJP approaches is that to esti-
741 mate the annual FFD under climate change conditions, a CS run of the RR

742 model is required in order to re-estimate the antecedent soil moisture con-
743 dition for the event-based RR model. The length of time the CS should be
744 run to capture the changes in the antecedent SM is indeterminate. One of
745 the advantages of the hybrid-CE approach is that it can easily be adapted
746 to assess impacts for climate change scenarios, since it needs only a short
747 CS to update the input information, i.e., the SM distribution and the POT
748 model parameters for the event-based RR model. Therefore it has the poten-
749 tial to provide unbiased efficient predictions under climate change conditions.

750

751 As mentioned in the introduction, CS has the greatest potential to pro-
752 vide reliable estimates of the FFD for both current and changed climate
753 scenarios, but is the most computationally expensive method, particularly
754 as RR models are likely to become complex in the future (e.g. TOPKAPI,
755 Hydrogeosphere). The hybrid-CE approach is approximately 100-1000 times
756 faster than the CS approach. Though the hybrid-CE approach does require
757 some additional calculations related to the EINEE and POT methods, the
758 additional computational time of these is minor compared to the compu-
759 tational efficiency from a 100 to 1000 times reduction in the runtime of a
760 complicated distributed rainfall-runoff model. This would further improve if
761 parallel computing was utilised, since event based approaches are far easier
762 to parallelise than a single long run of CS.

763

764 Given the conceptually sounder approach of using causative events and
765 the improved predictive accuracy compared with existing EB approaches,
766 and the vastly increased computational efficiency compared with the CS ap-

767 proach, the hybrid-CE approach ranks ahead of the other approaches for
768 estimating the annual FFD. However, there is still significant work required
769 to further develop the hybrid-CE approach in order to provide the practically
770 relevant estimates of floods in more realistic case-study catchments.

771

772 *5.2. Future development of the hybrid-CE method*

773 The advantages of the hybrid-CE method were demonstrated in this paper
774 using a simplified synthetic case study where the extreme daily flow volumes
775 were estimated. Future research will extend the hybrid-CE method to pro-
776 vide flood predictions for more realistic practical applications. Of primary
777 interest is estimating the instantaneous peak flood rate instead of the daily
778 flow volume. As mentioned in the previous section, this will require using a
779 more realistic subdaily rainfall model, that takes into account spatially and
780 temporally varying rainfall characteristics and a RR model that captures
781 spatial variability of catchment properties and runoff-routing at the subdaily
782 time steps. The EB component of the hybrid-CE model must be run for
783 the entire event duration, as opposed to a single time step. As the current
784 AMXJP method (Nathan et al. (2003)), already takes into account several
785 of these factors (seasonality, event duration modelling, temporal rainfall pat-
786 terns) these existing techniques will be incorporated into the hybrid-CE ap-
787 proach, tested and refined as necessary. These future extensions will enable
788 the hybrid-CE approach to provide more realistic predictions for practical
789 applications.

790

791 One of the major assumptions of all the derived flood frequency methods

792 is the ability of the rainfall model and RR model to properly capture the
793 dominant physical processes which produce extreme flood events. Inherent
794 in the development of any environmental model is the predictive uncertainty
795 produced by data errors and model structural uncertainty (refer to Thyer
796 et al. (2009) and Renard et al. (2010) for further discussions). These predic-
797 tion errors can be incorporated into the hybrid-CE approach, by modifying
798 Eq. (1) to be probabilistic rather than deterministic. Note the challenge is
799 how to specify this probabilistic description given the complex, heteroscedas-
800 tic and autocorrelated errors in hydrological model predictions. Research is
801 ongoing on developing robust approaches to handle these errors, see for ex-
802 ample Schoups and Vrugt (2010) and enhancements proposed by Evin et al.
803 (2013).

804

805 **6. Conclusions**

806 This paper has introduced a new hybrid causative event method for pro-
807 viding an efficient and robust estimation of annual flood frequency distribu-
808 tion. The method uses a short continuous simulation of the rainfall-runoff
809 process to provide inputs to an event-based approach for estimating the dis-
810 tribution of streamflow events at the time scale of interest. The peak over
811 threshold method is incorporated to convert this distribution to the annual
812 frequency distribution. It successfully combines the accuracy of continu-
813 ous simulation method with the efficiency of event-based methods. It takes
814 into account the joint probability nature of the rainfall-runoff process, which
815 overcomes the prediction errors induced by the assumptions of the widely

816 adopted design storm approach. The use of causative events provides a
817 conceptually sounder approach than the AMXJP method by avoiding the
818 reliance on arbitrary assumptions and compensatory errors. Significantly, it
819 reduces computational demand compared with a long continuous simulation
820 run of the rainfall-runoff model. The study reported here demonstrated the
821 advantages (more efficient and reliable predictions) of the hybrid causative
822 event approach over existing approaches using a simplified case study which
823 estimated extreme daily flow volumes. Future work will extend the hybrid
824 causative event approach to more realistic practical applications which esti-
825 mate extreme instantaneous peak flows, taking into account the spatially and
826 temporally varying characteristics of the rainfall and rainfall-runoff processes.

827

828 **Acknowledgements**

829 The RFortran (Thyer et al. (2011)) software package was used extensively
830 to speed the development and application of the methods presented in this
831 paper.

832

833 **Appendix: Efficient numerical integration for extreme events**

834 The procedure of the ENIEE method is outlined as follows:

835

- 836 1. The range of the streamflow Q values of interest is discretized into m
837 number of intervals. The mid points q_k of these intervals are extracted.

838

- 839 2. The ranges of the rainfall depth R and soil moisture amount S that are
840 causative to the streamflows of interest are discretized into n intervals
841 with increments of Δr and Δs , respectively. The mid points r_i and s_i
842 are extracted.
- 843
- 844 3. The outmost loop starts from the highest value of Q , namely, q_1 . For
845 q_1 , the inner loop also starts from the biggest value of R , i.e., r_1 . r_1
846 is combined with every possible S value s_j in the innermost loop to
847 produce a streamflow using the RR model.
- 848
- 849 4. The innermost loop also begins by first starting at the highest value
850 s_1 and search along the S values, until the smallest streamflow which
851 is greater than q_1 is found. The innermost loop is terminated at this
852 point and the corresponding s_j value is recorded and denoted as $s_T^{q_1, r_1}$.
- 853
- 854 5. The R loop continues to the next value r_2 and the terminating $s_T^{q_1, r_2}$ is
855 recorded likewise.
- 856
- 857 6. Step 5 moves on to the lower end of the R range until the smallest R
858 value which contributes to a streamflow that is greater than q_1 . The
859 loop of R is terminated and this R value is recorded and denoted as
860 $r_T^{q_1}$. Any R value that is smaller than $r_T^{q_1}$ will not produce a streamflow
861 that is greater than q_1 even it is combined with the biggest S value s_1 .
- 862

- 863 7. Then a set of the recorded S values $\mathbf{S}_T = (s_T^{q_1, r_1}, s_T^{q_1, r_2}, \dots, s_T^{q_1, r_T^{q_1}})$ cor-
864 responding to all the checked R values, i.e., $r_1, r_2, \dots, r_T^{q_1}$ is constructed.
865
- 866 8. The exceedance probability of q_1 is calculated using Eq. (3) for every
867 checked pair of (r_i, s_j) .
868
- 869 9. The Q loop moves on to q_2 . For each r_i value, steps 4 to 8 are repeated,
870 except that the starting point of the S loop is signified by the previ-
871 ously recorded $s_T^{q_1, r_i}$ and a new ending value $s_T^{q_2, r_i}$ for each r_i is recorded
872 to replace this entry in \mathbf{S}_T set for the next Q value to be checked.
873
- 874 10. As this procedure moves beyond the previously recorded $r_T^{q_1}$, the loop
875 of S starts from the very beginning, i.e., s_1 . The R loop continues until
876 the smallest R value $r_T^{q_2}$ that contributes to q_2 as described in step 5.
877 Thus the set \mathbf{S}_T is updated as $(s_T^{q_2, r_1}, s_T^{q_2, r_2}, \dots, s_T^{q_2, r_T^{q_2}})$.
878
- 879 11. The exceedance probability of q_2 is calculated using Eq. (3) for all the
880 checked combinations of R and S values in this run and added by the
881 exceedance probability of q_1 calculated before. As q_2 is less than q_1 , the
882 part of the probability exceeding q_1 does not need to be recalculated
883 for q_2 .
884
- 885 12. This procedure repeats for the rest of the Q values under study.
886

887 Fig. 11 illustrates this procedure. As one can see, as the evaluation moves
888 on to the lower end of Q range, the computation accelerates as all the calcu-
889 lations done for the previous Q values can be used.

890

Reference

- Bergström, S., 1995. The hbv model. In: Singh, V. P. (Ed.), Computer Models of Watershed Hydrology. Water Resources Publications, Highlands Ranch, CO., pp. 443–476.
- Brown, L. D., Cai, T. T., DasGupta, A., 2001. Interval estimation for a binomial proportion. *Stat. Sci.* 16 (2), 101–133.
- Calver, A., Lamb, R., April 1-3 2000. Generalised flood frequency estimation using continuous simulation. In: Bronstert, A., Bismuth, C. (Eds.), Proceedings of the European Conference on Advances in Flood Research. Potsdam, Germany, pp. 412–421.
- Camici, S., Tarpanelli, A., Brocca, L., Melone, F., Moramarco, T., 2011. Design soil moisture estimation by comparing continuous and storm-based rainfall-runoff modelling. *Water Resour. Res.* 47 (5), art. no. W05527.
- Cowperrwait, P. S., 2006. A spatial-temporal point process model of rainfall for the thames catchment, uk. *J. Hydrol.* 330 (3).
- Cunnane, C., 1973. A particular comparison of annual maxima and partial duration series methods of flood frequency prediction. *J. Hydrol.* 18, 257–271.

- Cunnane, C., 1979. A note on the poisson assumption in partial duration series models. *Water Resour. Res.* 15 (2), 489–494.
- Davis, P. J., Rabinowitz, P., 1975. *Methods of Numerical Integration*. Academic Press, New York.
- Eagleson, P. S., 1972. Dynamics of flood frequency. *Water Resour. Res.* 8 (4), 878–898.
- Evin, G., Kavetski, D., Thyer, M. and Kuczera, G., 2013. Pitfalls and improvements in the joint inference of heteroscedasticity and autocorrelation in hydrological model calibration. *Water Resour Res.* 49 (7), 4518–4524, <http://dx.doi.org/10.1002/wrcr.20284>.
- Hebson, C., Wood, E. F., 1982. A derived flood frequency distribution using horton order ratios. *Water Resour. Res.* 18 (5), 1509–1518.
- Heneker, T. M., Lambert, M. F. and Kuczera, G., 2001. A point rainfall model for risk-based design, *J. Hydrol.* 247 (1-2), 54–71.
- Henley, B. J., Thyer, M. A., Kuczera, G. and Franks, S. W., 2011, Climate-informed stochastic hydrological modeling: Incorporating decadal-scale variability using paleo data. *Water Resour. Res.* 47 (11), W11509.<http://dx.doi.org/10.1029/2010WR010034>.
- Hill, P., Mein, R. G., Weinmann, E., 1997. Development and testing of new design losses for south-eastern australia. In: Society, N. Z. H., on Water Engineering, A. N. C. (Eds.), *Proceedings of the 24th Hydrology and Water Resources Symposium*. Auckland, Newzealand.

- James, W., Robinson, M., April 8-11 1986. Continuous deterministic urban runoff modelling. In: Maksimovic, C., Radojkovic, M. (Eds.), Proceedings of the International Symposium on the Comparison of Urban Models with Real Catchment Data. Dubrovnik, Yugoslavia, pp. 347–378.
- Kuczera, G., Lambert, M., Heneker, T., Jennings, S., Frost, A., Coombes, P., November 10-13 2003. Joint probability and design storms at the crossroads. In: Boyd, M. (Ed.), About water: 28th International Hydrology and Water Resources Symposium. Wollongong, Australia.
- Laurenson, E. M., Mein, R. G., Nathan, R. J., 2010. RORB Version 6: Runoff Routing Program (User Manual). Monash University, Department of Civil Engineering in conjunction with Sinclair Knight Merz Pty. Ltd.
- Michele, D. C., Salvadori, G., 2002. On the derived flood frequency distribution: analytical formulation and the influence of antecedent soil moisture condition. *J. Hydrol.* 262 (1-4), 245–258.
- Moughamian, M. S., Mclauchlin, D. M., Bras, R. L., 1987. Estimation of flood frequency: an evaluation of two derived distribution procedures. *Water Resour. Res.* 23 (7), 1309–1319.
- Nathan, R., Weinmann, E., Hill, P., November 10-13 2003. Use of monte carlo simulation to estimate the expected probability of large to extreme floods. In: Boyd, M. (Ed.), About water: 28th International Hydrology and Water Resources Symposium. Wollongong, Australia.
- Neal, J., Fewtrell, T., Trigg, M., 2009. Parallelisation of storage cell flood models using openmp. *Environ. Modell. Softw.* 24, 872–877.

- Nelsen, R. B., 2006. *An Introduction to Copulas*. Springer.
- Peel, M., Chew, F., Weston, A., McMachon, T., 2000. Extension of unimpaired monthly streamflow data and regionalisation of parameter values to estimate streamflow in ungauged catchments. Report 37 pp, National Land and Water Resources Audit.
- Pilgrim, D. H., 1987. *Australian rainfall and runoff: a guide to flood estimation*. Barton, A.C.T.: Institute of Engineers, Australia.
- Qin, J., 2010. A high-resolution hierarchical model for space-time rainfall. Ph.D. thesis, The University of Newcastle.
- Rahman, A., Weinmann, P. E., Hoang, T. M. T., Laurenson, E. T., 2002. Monte carlo simulation of flood frequency curves from rainfall. *J. Hydrol.* 256 (3).
- Raines, T. H., Valdes, J. B., 1993. Estimation of flood frequencies for ungauged catchments. *J. Hydr. Engrg., ASCE*, 119 (10), 1138–1154.
- Renard, B., Kavetski, D., Kuczera, G., Thyer, M. and Franks, S. W., 2010. Understanding predictive uncertainty in hydrologic modelling: The challenge of identifying input and structural errors, *Water Resour. Res.*, 46 (5), W05521.<http://dx.doi.org/10.1029/2009WR008328>.
- Rosbjerg, D., 1987. On the annual maximum distribution in dependent partial duration series. *Stoch. Hydrol. Hydraul.* 1, 3–16.
- Rosbjerg, D., 1993. *Partial duration series in water resources*. Habilitation Thesis, Technical University of Denmark.

- Shane, R. M., Lynn, W. R., 1964. Mathematical model for flood risk evaluation. *J. Hydraul. Div., ASCE* (90), 1–20.
- Schoups, G. and Vrugt J. A., 2010. A formal likelihood function for parameter and predictive inference of hydrologic models with correlated, heteroscedastic, and non-Gaussian errors. *Water Resour. Res.* 46 (10), W10531.<http://dx.doi.org/10.1029/2009WR008933>
- Srikanthan, R., McMahon, T. A., 2001. Stochastic generation of annual, monthly and daily climate data. *Hydrol. Earth Syst. Sc.* 5 (4), 653–670.
- Therrien, R., McLaren, R. G., Sudicky, E. A., 2010. HydroGeoSphere: A three-dimensional numerical model describing fully-integrated subsurface and surface flow and solute transport. Groundwater Simulation Group.
- Thyer, M., Leonard, M., Kavetski, D., Need, S. and Renard, B. (2011). The open source RFortran library for accessing R from Fortran, with applications in environmental modelling. *Environ. Modell. Softw.* 26 (2), 219–234.
- Thyer, M., Renard, B., Kavetski, D., Kuczera, G., Franks, S. W., Srikanthan, S., 2009. Critical evaluation of parameter consistency and predictive uncertainty in hydrological modeling: A case study using bayesian total error analysis. *Water Resour. Res.* 45, doi:10.1029/2008WR006825.
- Todorovic, P., Zelenhasic, E., 1970. A stochastic model for flood analysis. *Water Resour. Res.* 6, 1641–1648.
- Vischel, T., Pegram, G., Sinclair, S., Parak, M., 2008. Implementation of the topkapi model in south africa: Initial results from the liebenbergsvlei catchment. *Water SA* 34 (3), 331–342.

Walsh, M., Pilgrim, D., Cordery, I., October 2-4 1991. Initial losses for design flood estimation in new south wales. In: 1991 International Hydrology and Water Resources Symposium: Challenges for Sustainable Development. Perth, Australia.

Weiss, L. L., 1964. Sequence of wet or dry days described by a markov chain probability model. Water Resour. Res. 92 (4), 169–176.

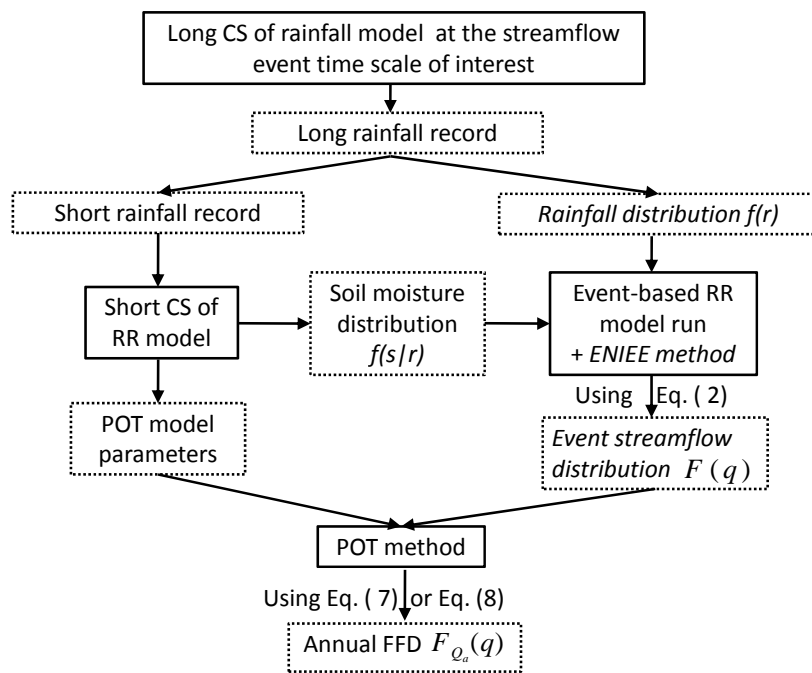


Figure 1: Flow chart showing the procedure of the hybrid-CE method.

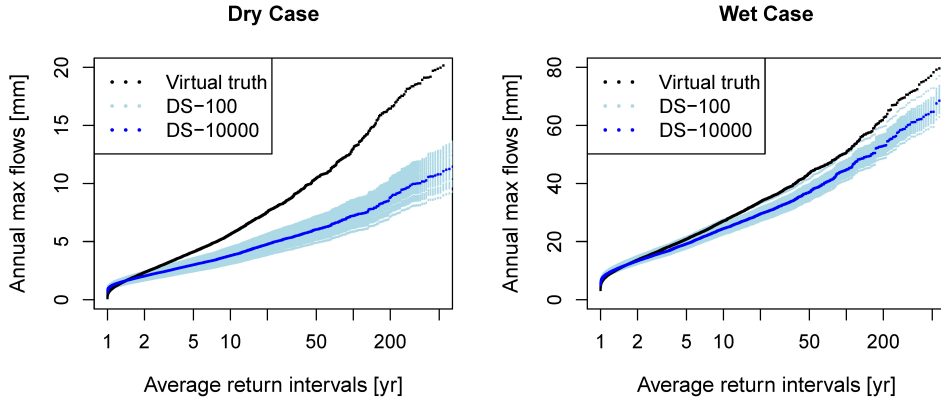


Figure 2: Results of the DS approach. Black curves indicate the virtual truth distributions, while the light blue curves indicate the predicted distributions using randomly sampled 100-yr synthetic records to derive 100 distributions of SM, to illustrate the impact of sampling error. The dark blue curves show the predicted distribution based on the SM values from the 10,000-yr synthetic records to illustrate the results free from sampling error.

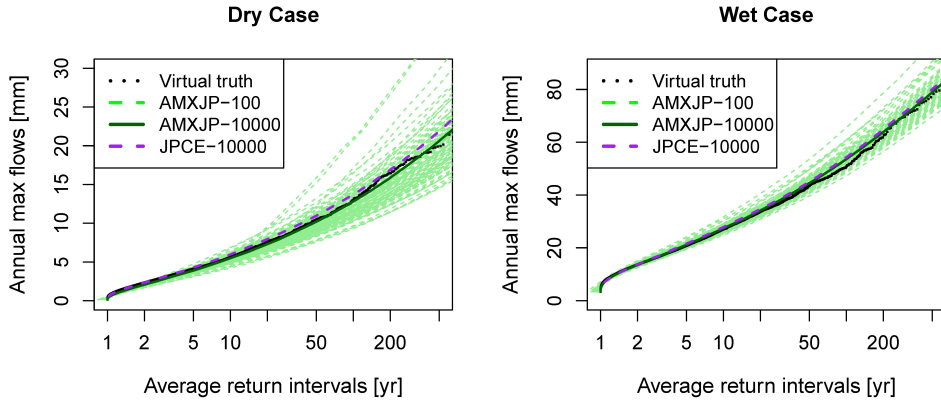


Figure 3: Results of the AMXJP approach. Black curves indicate the virtual truth distribution, light green curves the results of using randomly sampled 100-yr synthetic records to derive the SM distributions, dark green curves the results of using 10,000-yr synthetic records, purple curves the results of using causative input events.

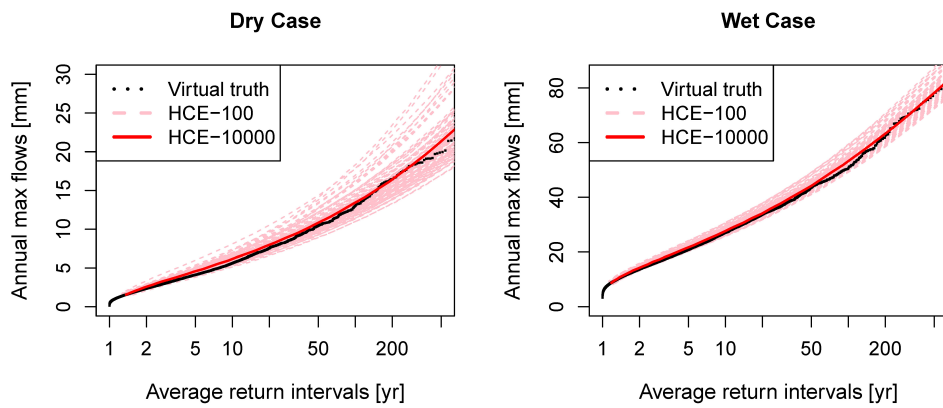


Figure 4: Results of the hybrid-CE method. Black curves indicate the virtual truth distribution. Pink curves show the results of using randomly sampled 100-yr synthetic records to assess the daily SM distributions and the POT model parameters, while red curves the results of using 10,000-yr CS results.

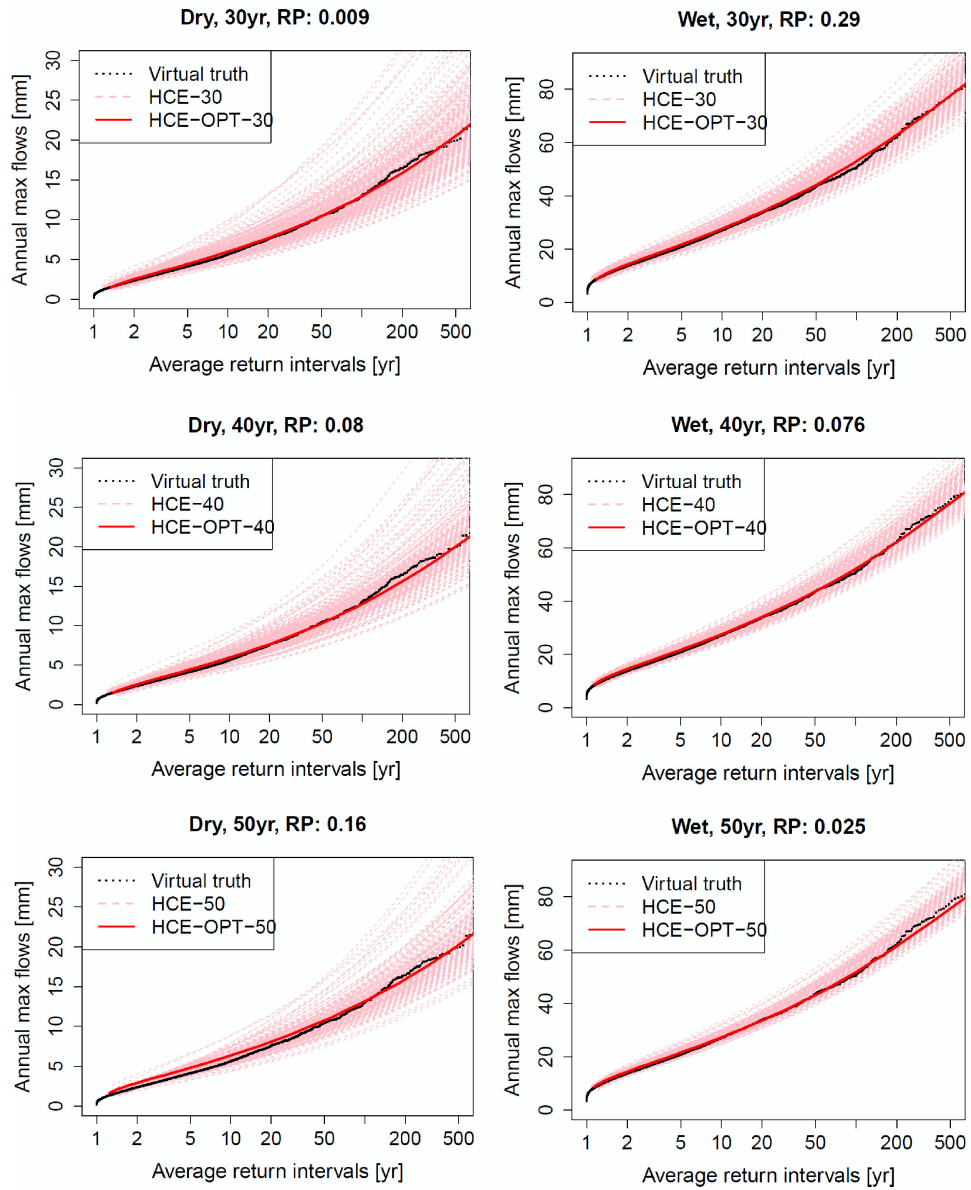


Figure 5: Prediction of results using the selected optimal short records. Black curves indicate the virtual truth distributions, pink curves the results using randomly sampled short records, red curves the results using the optimal short records. The values of RP indicate the % of the random samples outperform the optimal record.

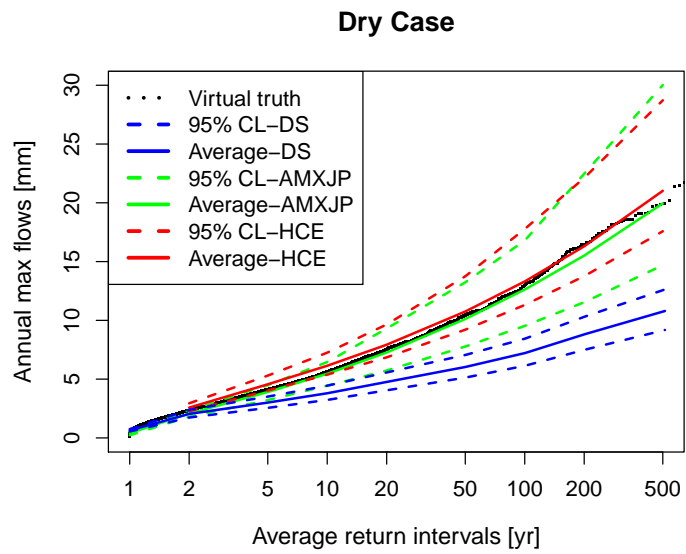


Figure 6: Comparison of the 95% confidence limits and averaged predictions of different methods for the dry case.

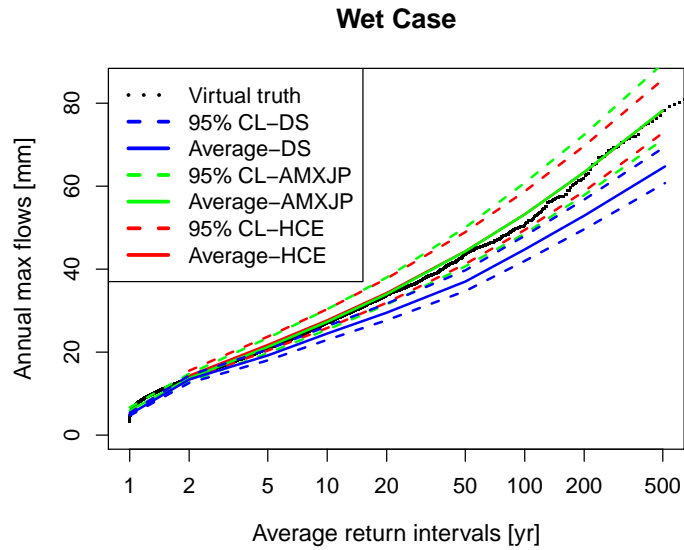


Figure 7: Comparison of the 95% confidence limits and averaged predictions of different methods for the wet case.

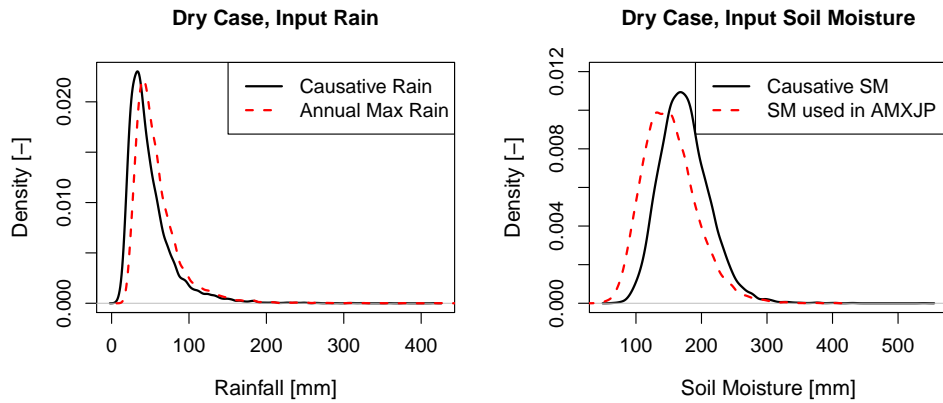


Figure 8: Comparison of the input distributions used in the AMXJP approach and the distributions of the causative events of annual maximum flows for the dry case.

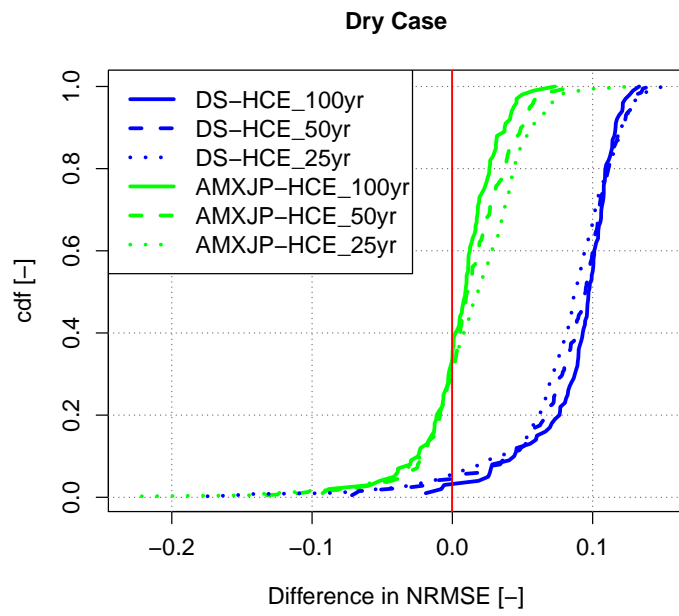


Figure 9: Comparison of NRMSE between DS and hybrid-CE method (DS-HCE), AMXJP and hybrid-CE methods (AMXJP-HCE) for different record lengths of the dry case.

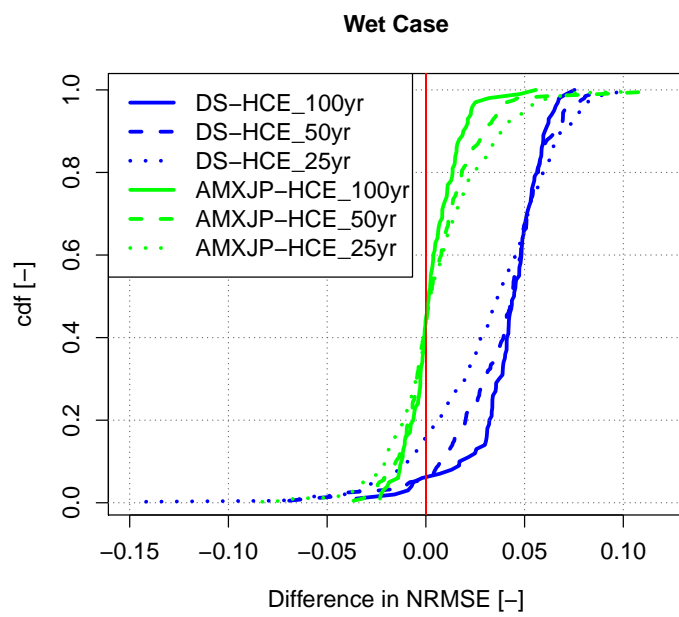


Figure 10: Comparison of NRMSE between DS and hybrid-CE methods (DS-HCE), AMXJP and hybrid-CE methods (AMXJP-HCE) for different record lengths of the wet case.

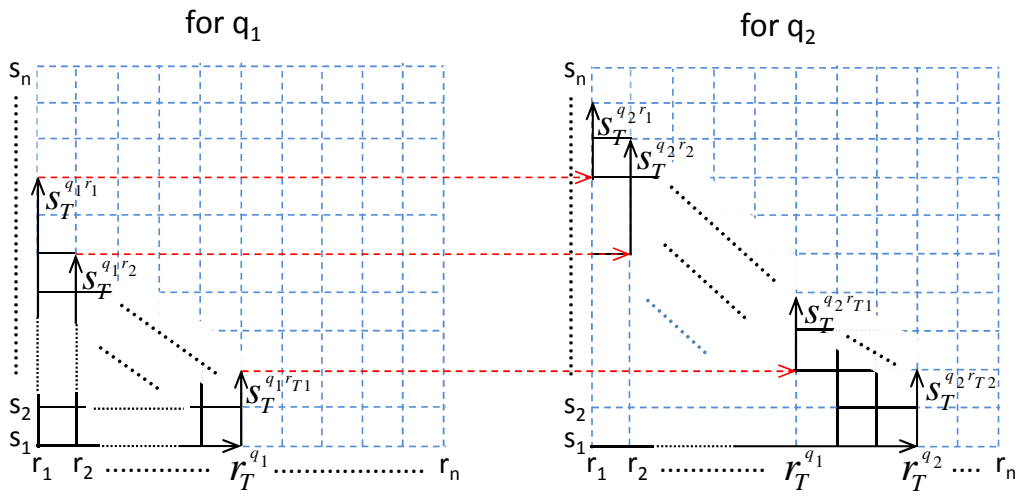


Figure 11: Illustration of the gridding procedure for the first two flow values. Black area indicates the grid points at which the RR model is evaluated and blue area the grid points that are unnecessary to be checked.